EUROPEAN ORGANIZATION FOR NUCLEAR RESEARCH

CERN–EP-Paper 300/Draft 1

29 January 2002

Measurement of Inclusive $f_1(1285)$ and $f_1(1420)$ Production in Z Decays with the DELPHI Detector

DELPHI Collaboration

Abstract

Inclusive production of two $(K\bar{K}\pi)^0$ states in the mass region 1.22–1.56 GeV in Z decays at LEP I has been observed by the DELPHI Collaboration. The measured masses and widths are 1274 ± 4 and 29 ± 12 MeV for the first peak and 1426 ± 4 and 51 ± 14 MeV for the second. A partial-wave analysis has been performed on the $(K\bar{K}\pi)^0$ spectrum in the mass range; the first peak is consistent with the quantum numbers $I^G(J^{PC}) = 0^+(0^{-+}/1^{++})$ and the second with $I^G(J^{PC}) = 0^+(1^{++})$. These measurements, as well as their total hadronic production rates per hadronic Z decay, are consistent with the mesons of the type $n\bar{n}$, where $n = \{u, d\}$. They are very likely to be the $f_1(1285)$ and the $f_1(1420)$, respectively.

(To be submitted to Phys.Lett.B)

Send comments up to xx/02/2002 to
Philippe.Gavillet@cern.ch,Mikhail.Chapkine@cern.ch, Augustin@lpnhep.in2p3.fr (Editor),
stocchi@lal.in2p3.fr,Dimartino@vxdel1.cern.ch

J.Abdallah[23], P.Abreu[21], W.Adam[48], P.Adzic[11], T.Albrecht[16], T.Alderweireld[2], R.Alemany-Fernandez[8], T.Allmendinger[16], P.P.Allport[22], S.Almehed[24], U.Amaldi[27], N.Amapane[43], S.Amato[45], E.Anashkin[34], A.Andreazza[26], S.Andringa[21], N.Anjos[21], P.Antilogus[25], W-D.Apel[16], Y.Arnoud[13], S.Ask[24], B.Asman[42], J.E.Augustin[23], A.Augustinus[8], P.Baillon[8], A.Ballestrero[43], P.Bambade[19], R.Barbier[25], D.Bardin[15], G.Barker[16], A.Baroncelli[37], M.Battaglia[8], M.Baubillier[23], K-H.Becks[50], M.Begalli[6], A.Behrmann[50], N.Benekos[30], A.Benvenuti[5], C.Berat[13], M.Berggren[23], L.Berntzon[42], D.Bertrand[2], M.Besancon[38], N.Besson[38], D.Bloch[9], M.Blom[29], M.Bonesini[27], M.Boonekamp[38], P.S.L.Booth[22], G.Borisov[8,20], O.Botner[46], B.Bouquet[19], T.J.V.Bowcock[22], I.Boyko[15], M.Bracko[41], R.Brenner[46], E.Brodet[33], P.Bruckman[17], J.M.Brunet[7], L.Bugge[31], P.Buschmann[50], M.Calvi[27], T.Camporesi[8], V.Canale[36], F.Carena[8], C.Carimalo[23], N.Castro[21], F.Cavallo[5], M.Chapkin[40], Ph.Charpentier[8], P.Checchia[34], R.Chierici[8], P.Chliapnikov[40], S.U.Chung[8], K.Cieslik[17], P.Collins[8], R.Contri[12], G.Cosme[19], F.Cossutti[44], M.J.Costa[47], B.Crawley[1], D.Crennell[35], J.Cuevas[32], J.D'Hondt[2], J.Dalmau[42], T.da Silva[45], W.Da Silva[23], G.Della Ricca[44], A.De Angelis[44], W.De Boer[16], C.De Clercq[2], B.De Lotto[44], N.De Maria[43], A.De Min[34], L.de Paula[45], L.Di Ciaccio[36], A.Di Simone[37], K.Doroba[49], J.Drees[50], M.Dris[30], G.Eigen[4], T.Ekelof[46], M.Ellert[46], M.Elsing[8], M.C.Espirito Santo[8], G.Fanourakis[11], D.Fassouliotis[11], M.Feindt[16], J.Fernandez[39], A.Ferrer[47], F.Ferro[12], U.Flagmeyer[50], H.Foeth[8], E.Fokitis[30], F.Fulda-Quenzer[19], J.Fuster[47], M.Gandelman[45], C.Garcia[47], Ph.Gavillet[8], E.Gazis[30], D.Gele[9], T.Geralis[11], R.Gokieli[8,49], B.Golob[41], G.Gomez-Ceballos[39], P.Goncalves[21], E.Graziani[37], G.Grosdidier[19], K.Grzelak[49], J.Guy[35], C.Haag[16], F.Hahn[8], S.Hahn[50], A.Hallgren[46], K.Hamacher[50], K.Hamilton[33], J.Hansen[31], S.Haug[31], F.Hauler[16], V.Hedberg[24], M.Hennecke[16], H.Herr[8], S-O.Holmgren[42], P.J.Holt[33], M.A.Houlden[22], K.Hultqvist[42], J.N.Jackson[22], Ch.Jarlskog[24], G.Jarlskog[24], P.Jarry[38], D.Jeans[33], E.K.Johansson[42], P.D.Johansson[42], P.Jonsson[25], C.Joram[8], L.Jungermann[16], F.Kapusta[23], S.Katsanevas[25], E.Katsoufis[30], R.Keranen[16], G.Kernel[41], B.P.Kersevan[8,41], A.Kiiskinen[14], B.T.King[22], N.J.Kjaer[8], P.Kluit[29], P.Kokkinias[11], C.Kourkoumelis[3], O.Kouznetsov[15], Z.Krumstein[15], M.Kucharczyk[17], J.Kurowska[49], B.Laforge[23], J.Lamsa[1], G.Leder[48], F.Ledroit[13], L.Leinonen[42], R.Leitner[28], J.Lemonne[2], G.Lenzen[50], V.Lepeltier[19], T.Lesiak[17], W.Liebig[50], D.Liko[8,48], A.Lipniacka[42], J.H.Lopes[45], J.M.Lopez[32], D.Loukas[11], P.Lutz[38], L.Lyons[33], J.MacNaughton[48], A.Malek[50], S.Maltezos[30], F.Mandl[48], J.Marco[39], R.Marco[39], B.Marechal[45], M.Margoni[34], J-C.Marin[8], C.Mariotti[8], A.Markou[11], C.Martinez-Rivero[39], J.Masik[28], N.Mastroyiannopoulos[11], F.Matorras[39], C.Matteuzzi[27], F.Mazzucato[34], M.Mazzucato[34], R.Mc Nulty[22], C.Meroni[26], W.T.Meyer[1], E.Migliore[43], W.Mitaroff[48], U.Mjoernmark[24], T.Moa[42], M.Moch[16], K.Moenig[8,10], R.Monge[12], J.Montenegro[29], D.Moraes[45], S.Moreno[21], P.Morettini[12], U.Mueller[50], K.Muenich[50], M.Mulders[29], L.Mundim[6], W.Murray[35], B.Muryn[18], G.Myatt[33], T.Myklebust[31], M.Nassiakou[11], F.Navarria[5], K.Nawrocki[49], S.Nemecek[28], R.Nicolaidou[38], P.Niezurawski[49], M.Nikolenko[15,9], A.Nygren[24], A.Oblakowska-Mucha[18], V.Obraztsov[40], A.Olshevski[15], A.Onofre[21], R.Orava[14], K.Osterberg[8], A.Ouraou[38], A.Oyanguren[47], M.Paganoni[27], S.Paiano[5], J.P.Palacios[22], H.Palka[17], Th.D.Papadopoulou[30], L.Pape[8], C.Parkes[22], F.Parodi[12], U.Parzefall[22], A.Passeri[37], O.Passon[50], L.Peralta[21], V.Perepelitsa[47], A.Perrotta[5], A.Petrolini[12], J.Piedra[39], L.Pieri[37], F.Pierre[38], M.Pimenta[21], E.Piotto[8], T.Podobnik[41], V.Poireau[38], M.E.Pol[6], G.Polok[17], P.Poropat[44], V.Pozdniakov[15], P.Privitera[36], N.Pukhaeva[2,15], A.Pullia[27], J.Rames[28], L.Ramler[16], A.Read[31], P.Rebecchi[8], J.Rehn[16], D.Reid[29], R.Reinhardt[50], P.Renton[33], F.Richard[19], J.Ridky[28], I.Ripp-Baudot[9], D.Rodriguez[39], A.Romero[43], P.Ronchese[34], E.Rosenberg[1], P.Roudeau[19], T.Rovelli[5], V.Ruhlmann-Kleider[38], D.Ryabtchikov[40], A.Sadovsky[15], L.Salmi[14], J.Salt[47], A.Savoy-Navarro[23], C.Schwanda[48], B.Schwering[50], U.Schwickerath[8], A.Segar[33], R.Sekulin[35], M.Siebel[50], A.Sisakian[15], G.Smadja[25], O.Smirnova[24], A.Sokolov[40], A.Sopczak[20], R.Sosnowski[49], T.Spassov[8], M.Stanitzki[16], A.Stocchi[19], J.Strauss[48], B.Stugu[4], M.Szczekowski[49], M.Szeptycka[49], T.Szumlak[18], T.Tabarelli[27], A.C.Taffard[22], F.Tegenfeldt[46], F.Terranova[27], J.Timmermans[29], N.Tinti[5], L.Tkatchev[15], M.Tobin[22], S.Todorovova[8], B.Tome[21], A.Tonazzo[27], P.Tortosa[47], P.Travnicek[28], D.Treille[8], G.Tristram[7], M.Trochimczuk[49], C.Troncon[26], I.A.Tyapkin[15], P.Tyapkin[15], S.Tzamarias[11], O.Ullaland[8], V.Uvarov[40], G.Valenti[5], P.Van Dam[29], J.Van Eldik[8], A.Van Lysebetten[2], N.van Remortel[2], I.Van Vulpen[29], G.Vegni[26], F.Veloso[21], W.Venus[35], F.Verbeure[2], P.Verdier[25], V.Verzi[36], D.Vilanova[38], L.Vitale[44], V.Vrba[28], H.Wahlen[50], A.J.Washbrook[22], C.Weiser[8], D.Wicke[8], J.Wickens[2], G.Wilkinson[33], M.Winter[9], M.Witek[17], G.Wolf[8], O.Yushchenko[40], A.Zalewska[17], P.Zalewski[49], D.Zavrtanik[41], N.I.Zimin[15], A.Zintchenko[15], Ph.Zoller[9], M.Zupan[11]

[1]Department of Physics and Astronomy, Iowa State University, Ames IA 50011-3160, USA
[2]Physics Department, Universiteit Antwerpen, Universiteitsplein 1, B-2610 Antwerpen, Belgium
and IIHE, ULB-VUB, Pleinlaan 2, B-1050 Brussels, Belgium
and Faculté des Sciences, Univ. de l'Etat Mons, Av. Maistriau 19, B-7000 Mons, Belgium
[3]Physics Laboratory, University of Athens, Solonos Str. 104, GR-10680 Athens, Greece
[4]Department of Physics, University of Bergen, Allégaten 55, NO-5007 Bergen, Norway
[5]Dipartimento di Fisica, Università di Bologna and INFN, Via Irnerio 46, IT-40126 Bologna, Italy
[6]Centro Brasileiro de Pesquisas Físicas, rua Xavier Sigaud 150, BR-22290 Rio de Janeiro, Brazil
and Depto. de Física, Pont. Univ. Católica, C.P. 38071 BR-22453 Rio de Janeiro, Brazil
and Inst. de Física, Univ. Estadual do Rio de Janeiro, rua São Francisco Xavier 524, Rio de Janeiro, Brazil
[7]Collège de France, Lab. de Physique Corpusculaire, IN2P3-CNRS, FR-75231 Paris Cedex 05, France
[8]CERN, CH-1211 Geneva 23, Switzerland
[9]Institut de Recherches Subatomiques, IN2P3 - CNRS/ULP - BP20, FR-67037 Strasbourg Cedex, France
[10]Now at DESY-Zeuthen, Platanenallee 6, D-15735 Zeuthen, Germany
[11]Institute of Nuclear Physics, N.C.S.R. Demokritos, P.O. Box 60228, GR-15310 Athens, Greece
[12]Dipartimento di Fisica, Università di Genova and INFN, Via Dodecaneso 33, IT-16146 Genova, Italy
[13]Institut des Sciences Nucléaires, IN2P3-CNRS, Université de Grenoble 1, FR-38026 Grenoble Cedex, France
[14]Helsinki Institute of Physics, HIP, P.O. Box 9, FI-00014 Helsinki, Finland
[15]Joint Institute for Nuclear Research, Dubna, Head Post Office, P.O. Box 79, RU-101 000 Moscow, Russian Federation
[16]Institut für Experimentelle Kernphysik, Universität Karlsruhe, Postfach 6980, DE-76128 Karlsruhe, Germany
[17]Institute of Nuclear Physics,Ul. Kawiory 26a, PL-30055 Krakow, Poland
[18]Faculty of Physics and Nuclear Techniques, University of Mining and Metallurgy, PL-30055 Krakow, Poland
[19]Université de Paris-Sud, Lab. de l'Accélérateur Linéaire, IN2P3-CNRS, Bât. 200, FR-91405 Orsay Cedex, France
[20]School of Physics and Chemistry, University of Landcaster, Lancaster LA1 4YB, UK
[21]LIP, IST, FCUL - Av. Elias Garcia, 14-1^{o}, PT-1000 Lisboa Codex, Portugal
[22]Department of Physics, University of Liverpool, P.O. Box 147, Liverpool L69 3BX, UK
[23]LPNHE, IN2P3-CNRS, Univ. Paris VI et VII, Tour 33 (RdC), 4 place Jussieu, FR-75252 Paris Cedex 05, France
[24]Department of Physics, University of Lund, Sölvegatan 14, SE-223 63 Lund, Sweden
[25]Université Claude Bernard de Lyon, IPNL, IN2P3-CNRS, FR-69622 Villeurbanne Cedex, France
[26]Dipartimento di Fisica, Università di Milano and INFN-MILANO, Via Celoria 16, IT-20133 Milan, Italy
[27]Dipartimento di Fisica, Univ. di Milano-Bicocca and INFN-MILANO, Piazza della Scienza 2, IT-20126 Milan, Italy
[28]IPNP of MFF, Charles Univ., Areal MFF, V Holesovickach 2, CZ-180 00, Praha 8, Czech Republic
[29]NIKHEF, Postbus 41882, NL-1009 DB Amsterdam, The Netherlands
[30]National Technical University, Physics Department, Zografou Campus, GR-15773 Athens, Greece
[31]Physics Department, University of Oslo, Blindern, NO-0316 Oslo, Norway
[32]Dpto. Fisica, Univ. Oviedo, Avda. Calvo Sotelo s/n, ES-33007 Oviedo, Spain
[33]Department of Physics, University of Oxford, Keble Road, Oxford OX1 3RH, UK
[34]Dipartimento di Fisica, Università di Padova and INFN, Via Marzolo 8, IT-35131 Padua, Italy
[35]Rutherford Appleton Laboratory, Chilton, Didcot OX11 OQX, UK
[36]Dipartimento di Fisica, Università di Roma II and INFN, Tor Vergata, IT-00173 Rome, Italy
[37]Dipartimento di Fisica, Università di Roma III and INFN, Via della Vasca Navale 84, IT-00146 Rome, Italy
[38]DAPNIA/Service de Physique des Particules, CEA-Saclay, FR-91191 Gif-sur-Yvette Cedex, France
[39]Instituto de Fisica de Cantabria (CSIC-UC), Avda. los Castros s/n, ES-39006 Santander, Spain
[40]Inst. for High Energy Physics, Serpukov P.O. Box 35, Protvino, (Moscow Region), Russian Federation
[41]J. Stefan Institute, Jamova 39, SI-1000 Ljubljana, Slovenia and Laboratory for Astroparticle Physics,
Nova Gorica Polytechnic, Kostanjeviska 16a, SI-5000 Nova Gorica, Slovenia,
and Department of Physics, University of Ljubljana, SI-1000 Ljubljana, Slovenia
[42]Fysikum, Stockholm University, Box 6730, SE-113 85 Stockholm, Sweden
[43]Dipartimento di Fisica Sperimentale, Università di Torino and INFN, Via P. Giuria 1, IT-10125 Turin, Italy
[44]Dipartimento di Fisica, Università di Trieste and INFN, Via A. Valerio 2, IT-34127 Trieste, Italy
and Istituto di Fisica, Università di Udine, IT-33100 Udine, Italy
[45]Univ. Federal do Rio de Janeiro, C.P. 68528 Cidade Univ., Ilha do Fundão BR-21945-970 Rio de Janeiro, Brazil
[46]Department of Radiation Sciences, University of Uppsala, P.O. Box 535, SE-751 21 Uppsala, Sweden
[47]IFIC, Valencia-CSIC, and D.F.A.M.N., U. de Valencia, Avda. Dr. Moliner 50, ES-46100 Burjassot (Valencia), Spain
[48]Institut für Hochenergiephysik, Österr. Akad. d. Wissensch., Nikolsdorfergasse 18, AT-1050 Vienna, Austria
[49]Inst. Nuclear Studies and University of Warsaw, Ul. Hoza 69, PL-00681 Warsaw, Poland
[50]Fachbereich Physik, University of Wuppertal, Postfach 100 127, DE-42097 Wuppertal, Germany

1 Introduction

The inclusive production of mesons has been a subject of long-standing study at LEP [1,2], as it provides insight into the nature of fragmentation of quarks and gluons to hadrons. So far studies have been done on the S-wave mesons (both ${}^1S_0$ and ${}^3S_1$) such as π and ρ, as well as certain P-wave mesons $f_2(1270)$ and $K_2^*(1430)$ (i.e. ${}^3P_2$) and $f_0(980)$ and $a_0(980)$ (${}^3P_0$). Very little is known about the production of mesons belonging to other P-wave mesons (i.e. ${}^3P_1$ and ${}^1P_1$). For the first time, we present in this paper a study of the inclusive production of two $J^{PC} = 1^{++}$ mesons, the $f_1(1285)$ and the $f_1(1420)$ (i.e. ${}^3P_1$).

There are at least four nonstrange isoscalar mesons [3], $I^G(J^{PC}) = 0^+(1^{++})$ and $I^G(J^{PC}) = 0^+(0^{-+})$, known in the mass region between 1.2 and 1.5 GeV, which couple strongly to the decay channel $(K\bar{K}\pi)^0$. They are $f_1(1285)$, $\eta(1295)$, $f_1(1420)$ and $\eta(1440)$. All are seen prominently in the peripheral production from $\pi^- p$ interactions [3], indicating that, despite their decay into $(K\bar{K}\pi)^0$, they are mostly $n\bar{n}$ states, where $n = \{u, d\}$. There exist possibly two additional states, $I^G(J^{PC}) = 0^-?(1^{+-})\ h_1(1380)$ and $I^G(J^{PC}) = 0^+(1^{++})\ f_1(1510)$, which may harbor a large $s\bar{s}$ content, as they are produced with considerable cross sections in the peripheral reactions involving $K^- p$ interactions [3]. Given this complexity in the $(K\bar{K}\pi)^0$ systems, it is important that one seek answers as to which resonances among these are readily excited in inclusive hadron Z decays.

The DELPHI data for this study is based on the neutral $K\bar{K}\pi$ channel in the reaction

$$Z \to (K_S K^{\pm}\pi^{\mp}) + X^0 \tag{1}$$

Section 2 is devoted to the selection process for the event sample collected for this study. Sections 3 deals with a study of the $K\bar{K}\pi$ mass spectra. It is shown that selecting events with low mass $M(K_S K^{\pm})$ is the sensitive criteria to reveal the presence of two signals in the $f_1(1285)$ and $f_1(1420)$ mass region. A partial-wave analysis has been carried out to explore the spin-parity content of the two signals. It is presented in Section 4. A discussion of the results and conclusions are given in Sections 5 and 6.

2 Experimental Procedure

The analysis presented here is based on a data sample of 3392400 hadronic Z decays collected from 1992 to 1995 with the DELPHI detector. Detailed description of the DELPHI detector and its performance can be found elsewhere [4,5].

The charged particle tracks have been measured in the 1.2-T magnetic field by a set of tracking detectors. The average momentum resolution for charged particles in hadronic final states, $\Delta p/p$, is usually between 0.001 and 0.01, depending on their momentum as well as which detectors are included in the track fit.

A charged particle has been accepted in this analysis—if its momentum p is greater than 100 MeV/c; its momentum error Δp is less than p; and its impact parameter with respect to the nominal crossing point is within 4 cm in the transverse (xy) plane and 4 cm/$\sin\theta$ along the beam direction (z-axis), θ being the polar angle of the track.

Hadronic events are then selected by requiring at least 5 charged particles, with at least 3-GeV charged energy in each hemisphere of the event—defined with respect to the beam direction—and total charged energy at least 12% of the center-of-mass energy. The contamination from events due to beam-gas scattering and to γ-γ interactions is estimated to be less than 0.1% and the background from $\tau^+\tau^-$ events less than 0.2% of the accepted events.

After the event selection, in order to ensure a better signal-to-background ratio for the resonances in the $K_S K^{\pm}\pi^{\mp}$ invariant mass spectra, tighter requirements have been imposed on the track impact parameters with respect to the nominal crossing point, i.e. they have to be within 0.2 cm in the transverse plane and 0.4 cm/$\sin\theta$ along the beam direction.

$K^{\pm}$ identification has been provided by the Ring Imaging Cherenkov (RICH) detectors for particles with momenta above 700 MeV/c, while the ionization loss measured in the Time Projection Chamber (TPC) has been used for momenta above 100 MeV/c. The corresponding identification tags are based on the combined probabilities, derived from the average Cherenkov angle and the number of observed photons in the RICH detectors, as well as the measured $\mathrm{d}E/\mathrm{d}x$ in the TPC. Cuts on the tags have been applied to achieve the best signal-to-background ratio, while rejecting $e^{\pm}$, $\mu^{\pm}$, p and $\bar{p}$ tracks. A more detailed description of the identification tags can be found in Ref. [1]. In the present case, the $K^{\pm}$ identification efficiency has been estimated by comparing the $\phi(1020) \rightarrow K^+K^-$ signal in the experimental data with the simulated events generated with JETSET [6]—tuned with the DELPHI parameters [7]—and passed through the detector simulation program DELSIM [8]. Agreement within 4% is observed between the data and the simulation.

The K_S candidates are detected by their decay in flight into $\pi^+\pi^-$. The details of the method and the various cuts applied are described in Ref. [9]. Our selection process consists of taking the V^0's passing certain criteria for quality of the reconstruction plus a mass cut given by $0.45 < M(K_S) < 0.55$ GeV.

After all the above cuts, only events with at least one $K_S K^+\pi^-$ or $K_S K^-\pi^+$ combination have been kept in the present analysis, corresponding to a sample of 546 571 events.

3 $K_S K^{\pm}\pi^{\mp}$ Mass Spectra

A histogram of the $K_S\, K^{\pm}\, \pi^{\mp}$ mass spectrum is shown in Fig. 1. Also shown in the figure is the same mass spectrum with a $K^*(892)$ cut ($0.822 < M(K\pi) < 0.962$ GeV), which would be appropriate if the decay of a resonance had proceeded through a $K^*(892)$ intermediate state. Neither histogram shows visible enhancement in the mass region between 1.25 to 1.45 GeV.

This is due to the enormous background in this mass region coming from the high number of $K_S K^{\pm}\pi^{\mp}$ combinations ($\simeq \langle 9 \rangle$) per event in inclusive Z decays. The key to a successful study of the $f_1(1285)$ and $f_1(1420)$—under the circumstances—is to select events with low $M(K_S\, K^{\pm})$. This has the effect of selecting both the decay mode $a_0(980)^{\pm}\pi^{\mp}$ while reducing substantially the general background for the $K\bar{K}\pi$ system, and the interference region of the two $K^*(892)$ bands on the Dalitz plot. Varying this cut on MC generated events (see below) has led to choose a mass cut $M(K_S\, K^{\pm}) \leq 1.04$ GeV to maximize both $f_1(1285)$ and $f_1(1420)$ signals over background. The application of this cut on the experimental data is shown in Fig. 2, where two clear peaks are now seen in this mass region.

In order to measure the resonance parameters for these two states, we have generated a Monte Carlo sample, which was then passed through the standard detector simulation program. To estimate the background we have removed all mesons with a major decay mode into $(K\bar{K}\pi)^0$ in the mass region 1.25 to 1.45 GeV, i.e. $f_1(1285)$, $h_1(1380)$ and $f_1(1420)$, The smooth curve shown in Fig. 2 has been obtained by fitting the mass spectrum of the aforementioned MC sample between 1.15 to 1.65 GeV with a background

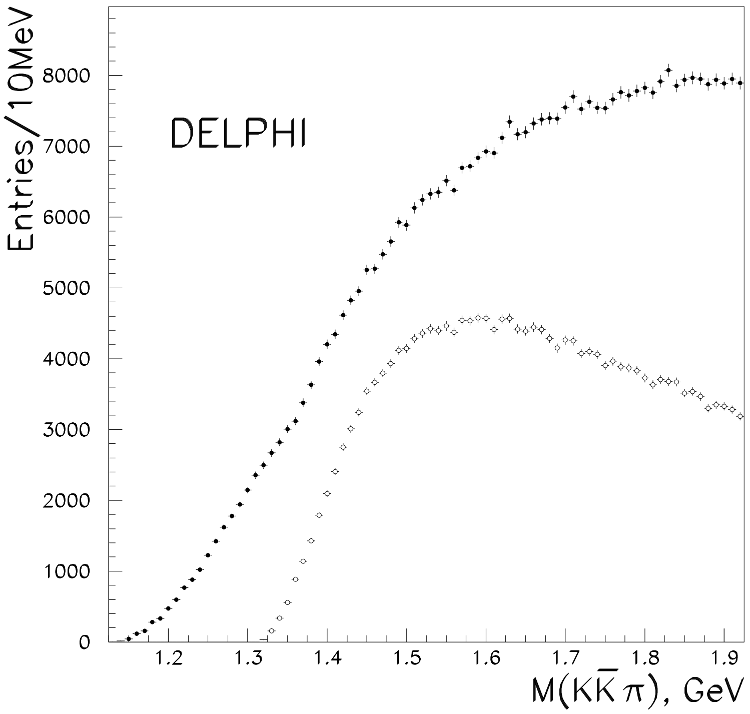

Figure 1: $M(K_s\, K^{\pm}\, \pi^{\mp})$ distributions from the Z decays with the DELPHI detector at LEP I. The histogram with solid (open) circles is for the full data sample (with a K^* cut $0.822 < M(K\pi) < 0.962$ GeV).

function

$$f_b(M) = (M - M_0)^{\alpha_1}\ \exp(\alpha_2\, M + \alpha_3\, M^2) \tag{2}$$

where M and M_0 are the effective masses of the $(K\bar{K}\pi)^0$ system and its threshold, respectively, and α_i are the experimental parameters. We have fitted the $(K\bar{K}\pi)^0$ spectrum adding two S-wave Breit-Wigner forms to the background $f_b(M)$, given by

$$f_r(M) = \frac{\Gamma_r^2}{(M - M_r)^2 + (\Gamma_r/2)^2} \tag{3}$$

where M_r and Γ_r are the mass and the width to be determined experimentally. The
61 results are shown in Fig. 2 and also in Table I.

Table I. Fitted parameters and numbers of events

Mass (MeV)	Width (MeV)	Events
1274 ± 4	29 ± 12	$345 \pm 88\,(\text{stat}) \pm 69\,(\text{sys})$
1426 ± 4	51 ± 14	$790 \pm 119\,(\text{stat}) \pm 110\,(\text{sys})$

The main sources of systematic errors come from the various cuts and selection criteria applied for the V^0 reconstruction plus the charged K identification—on the one hand—and the conditions of the mass-fit procedure—on the other. To estimate the first type of error, we have compared the $K_s K^\pm$ mass distributions of the simulated sample with the real data. Normalized to the same number of events, both distributions agree within 7%, in the low $K_s K^\pm$ mass region.

The $f_1(1285)$ and $f_1(1420)$ signals show up over a large background ($\sim 80\%$). Variations of the background shape and amplitude thus induce sizable fluctuations of the fitted numbers of signal events, especially in the $f_1(1420)$ mass region. To quantify this effect, we have performed a series of fits, varying both the shape and the mass range of the fit, thereby allowing the background level to fluctuate. In this way we estimate the fit uncertainty to be 15% for the $f_1(1285)$ and 14% for the $f_1(1420)$. The systematic errors have been added quadratically and are shown in Table 1. It should be emphasized that the masses and the widths quoted in the table are not intended to be new experimental measurements; rather, they are merely given as an indication that our peaks are consistent with the known parameters. An in-depth analysis of such a measurement must include a relativistic Breit-Wigner form with a mass-dependent partial width which includes orbital angular-momentum barrier factors. In addition, one must consider the possibility that there can be more than one resonance of different spin-parity in each mass peak. Given the high level of background in our data sample, such an analysis—we believe—is not warranted at this time.

The overall experimental efficiencies for the two states are

$$\begin{array}{ccccc} (0.063 & \pm & 0.003)\% & \text{for} & f_1(1285) \\ (0.45 & \pm & 0.02)\% & \text{for} & f_1(1420) \end{array} \tag{4}$$

The quoted numbers include the following corrections for the $f_1(1285)$ and $f_1(1420)$ respectively: branching ratios to $K\bar{K}\pi$ $(0.09, 1.)$, fractions of final states with charged pion $(1/2, 2/3)$, branching ratio of $K^0 \to \pi^+\pi^- = 1/2 \times 0.686 = 0.343$, reconstruction and identification efficiency for the selected events $(0.058, 0.061)$ and $M(K_s\, K^\pm) \leq 1.04$ GeV mass cut correction factor $(0.70, 0.32)$.

4 Partial-wave Analysis

There exists a long list of 3-body partial-wave analyses; the reader may consult PDG [3] for earlier references, for example, on $a_1(1260)$, $a_2(1320)$, $K_1(1270/1400)$ or $K_2(1770)$. For the first time, we apply the same technique to a study of the $(K\bar{K}\pi)^0$ system from the inclusive decay of the Z at LEP.

A short introductory remark may be in order, for the general principles involved in a spin-parity analysis of the system composed of three pseudoscalars. The description of such a system requires five variables, which may be chosen to be the three Euler angles describing the orientation of the 3-body system in its suitably-chosen rest frame and two effective masses describing the decay Dalitz plot. We have chosen to employ the so-called Dalitz plot analysis, integrating over the three Euler angles. This entails an essential simplification in the number of parameters required in the analysis, as the decay amplitudes involving the D-functions defined over the three Euler angles and their appropriate decay-coupling constants, are orthogonal for different spins and parities [10]. The actual fitting of the data is done by using the maximum-likelihood method, in which the normalization integrals are evaluated with the accepted Monte Carlo events [11], thus taking into account the finite acceptance of the detector and the event selection.

The background under the two f_1's is very large, some $\sim$ 80%. It is assumed that this represents essentially different processes with, for example, different overall multiplicities—so that the background does not interfere with the signals. We assume further that the background itself is a non-interfering superposition of a flat distribution (on the Dalitz plot) and the partial waves $I^G(J^{PC}) = 0^+(1^{++})\, a_0(980)\pi$, $0^+(1^{++})\,(K^*(892)\bar{K} + c.c.)$ and $0^-(1^{+-})\,(K^*(892)\bar{K} + c.c.)$. We have verified that these amplitudes give a good description of the three background regions for $M(K\bar{K}\pi)$ in $1.22 \to 1.26$, $1.30 \to 1.38$ and $1.48 \to 1.56$ GeV, respectively.

The signal regions, for $M(K\bar{K}\pi)$ in $1.26 \to 1.30$ and $1.38 \to 1.48$ GeV, have been fitted with a non-interfering superposition of the partial waves $I^G(J^{PC}) = 0^+(1^{++})$, $0^+(1^{+-})$ and $0^-(0^{-+})$, where the decay channels $a_0(980)\pi$ and $K^*(892)\bar{K} + c.c.$ are allowed to interfere within a given J^{PC}. All other possible partial waves have been found to be negligible in the signal regions. The fit results can be summarized as follows: (1) the maximum likelihood is found to be the same for $I^G(J^{PC}) = 0^+(1^{++})\, a_0(980)\pi$ and for $0^-(0^{-+})\, a_0(980)\pi$, i.e. the 1.28- GeV region is equally likely to be the $f_1(1285)$ or the $\eta(1295)$; (2) in the 1.4-GeV region, the maximum likelihood is significantly better (by about 14 for $\Delta \ln \mathcal{L}$) for $I^G(J^{PC}) = 0^+(1^{++})$ $f_1(1420)$ than $I^G(J^{PC}) = 0^+(0^{-+})$ which excludes the $\eta(1440)$. The $I^G(J^{PC}) = 0^+(1^{+-})$ $h_1(1380)$ is also ruled out in this analysis (by about 23 for $\Delta \ln \mathcal{L}$).

The results of the partial-wave analysis are summarized in Fig. 3. It should be emphasized that both the mass-dependent (per 20 MeV) and the mass-independent global fits give compatible results. The masses, the widths and the numbers of events found in the mass-independent global fit, shown as solid curves in Fig. 3, are statistically consistent with those given in Table I, even though the overall background shape—see the dotted curve just below the histogram with error bars—exhibits a slight dip around 1.4 GeV which is *not present* in Fig. 2.

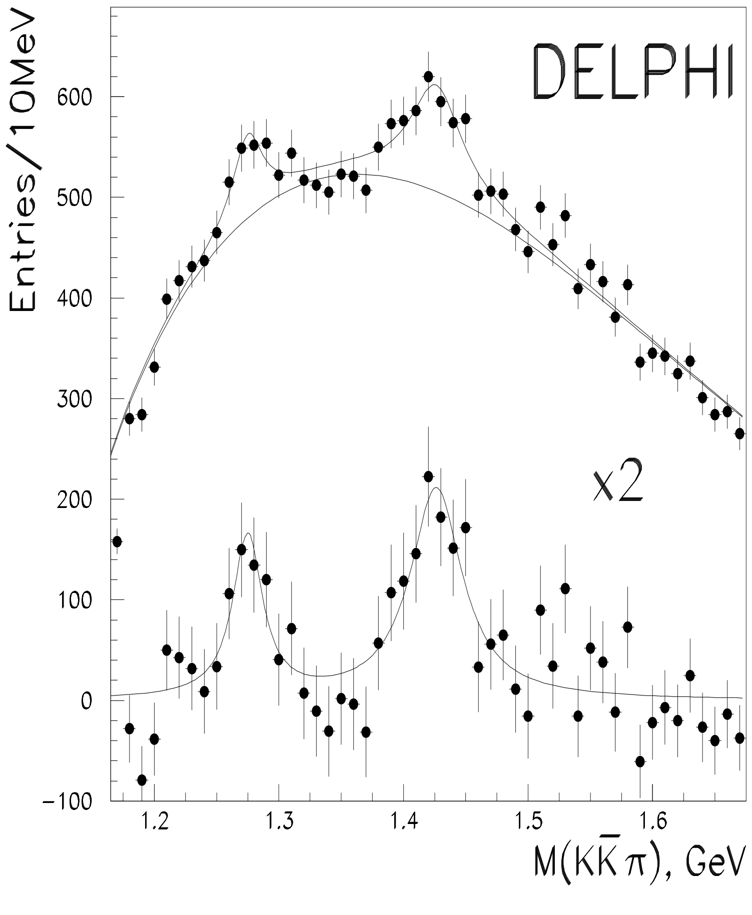

Figure 2: The same as in Fig. 1 but with a mass cut $M(K_s\,K^{\pm}) < 1.04$ GeV. The two solid curves in the upper part of the histogram describe Breit-Wigner fits over a smooth background (see text). The lower histogram and the solid curve give the same fits with the background subtracted and amplified by a factor of two.

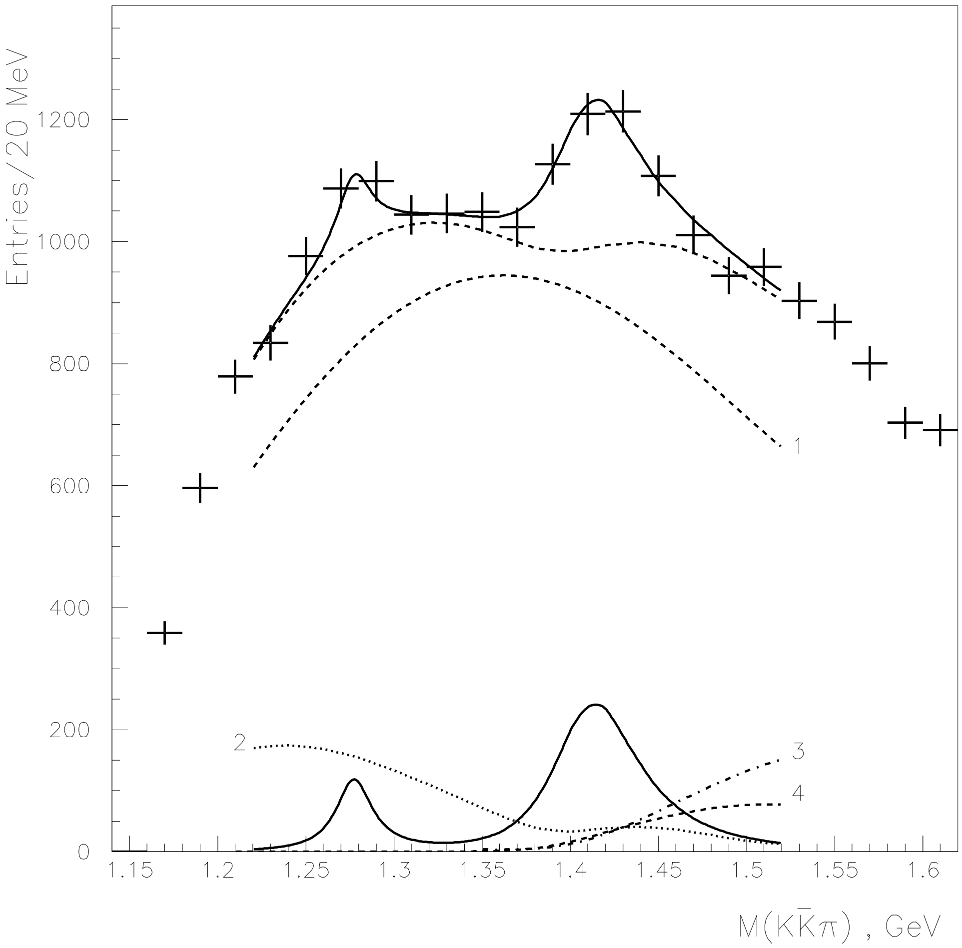

Figure 3: $M(K_s\,K^{\pm}\,\pi^{\mp})$ distributions per 20 MeV with a breakdown into the partial-waves for the signals and the background. The signals consist of $1^{++}\,a_0(980)\pi$ for the first peak and $1^{++}\,K^*(892)\bar{K}$ for the second peak. The background consists of non-interfering superposition of isotropic distribution (1), $1^{++}\,a_0(980)\pi$ (2), $1^{++}\,K^*(892)\bar{K}$ (3) and $1^{+-}\,K^*(892)\bar{K}$ (4).

5 Discussion

We have measured the production rate $\langle n\rangle$ per hadronic Z decay for $f_1(1285)/\eta(1295)$ and $f_1(1420)$. We assume for this study that *both have spin 1.* The results are

$$\begin{aligned}\langle n\rangle &= 0.159 \pm 0.051 \quad \text{for} \quad f_1(1285)\\ \langle n\rangle &= 0.0512 \pm 0.0105 \quad \text{for} \quad f_1(1420)\end{aligned} \tag{5}$$

taking a $K\bar{K}\pi$ branching ratio of $(9.0 \pm 0.4)\%$ for the $f_1(1285)$ and 100% for the $f_1(1420)$ [3]. The production rate per spin state [i.e. divided by $(2J+1)$] has been studied in Ref. [2]; in Fig. 4 is given all the available data for those mesons with a 'triplet' $q\bar{q}$ structure, i.e. $S = 1$ in the spectroscopic notation $^{2S+1}L_J$. To this figure we have added our two mesons for comparison. It is seen that both $f_1(1285)$ and $f_1(1420)$ come close to the line corresponding to other mesons whose constituents are thought to be of the type $n\bar{n}$. This is suggestive of two salient facts: (1)the first peak at 1.28 GeV is very likely to be the $f_1(1285)$; (2) both $f_1(1285)$ and $f_1(1420)$ have little $s\bar{s}$ content. Indeed, the two states which are thought to be pure $s\bar{s}$ mesons, the ϕ and the $f_2'(1525)$, are down by a factor $\gamma^k \approx 1/4$ ($\gamma = 0.50 \pm 0.02$ and $k = 2$, k being the number of s and $\bar{s}$ quarks in the meson), as shown in Fig. 4. This is highly unlikely given the production rate (5). For completeness, we give in Fig. 5 and in Table II the $f_1(1285)$ and $f_1(1420)$ differential cross sections as a function of the scaled momentum x_p, for $x_p > .05$ as the signal to background ratio is too small for lower momenta. Comparison with JETSET predictions is not possible in a meaningful way as there was no tuning for $f_1(1285)$ and $f_1(1420)$ and furthermore the implementation of the $(K\bar{K}\pi)^0$ decay of both resonances in JETSET is according to phase space thus not according to the correct matrix element.

Table II. Measured production rates per hadronic event and differential cross sections for the $f_1(1285)$ and $f_1(1420)$. The errors are the quadratic sum of statistical and systematic uncertainties

x_p range	$f_1(1285)$ rate	$(1/\sigma)(d\sigma/dx_p)$
.05-.10	0.0555±0.0235	1.110±0.470
.10-.20	0.0469±0.0188	0.469±0.188
.20-1.0	0.0503±0.0211	0.063±0.026
x_p range	$f_1(1420)$ rate	$(1/\sigma)(d\sigma/dx_p)$
.05-.10	0.0151±0.0045	0.302±0.090
.05-.10	0.0153±0.0038	0.153±0.038
.20-1.0	0.0180±0.0062	0.022±0.008

6 Conclusions

We have studied the inclusive production of $f_1(1285)/\eta(1295)$ and $f_1(1420)$ in Z decays at LEP I. The measured masses and widths are 1274 ± 4 and 29 ± 12 MeV for the first peak and 1426 ± 4 and 51 ± 14 MeV for the second one. For the first time, a partial-wave analysis has been carried out on the $(K\bar{K}\pi)^0$ system. The results show that the first peak is equally likely to be the $f_1(1285)$ or the $\eta(1295)$, while the second peak is consistent with the $f_1(1420)$. However, the hadronic production rate of these two states suggests that their quantum numbers are very probably $I^G(J^{PC}) = 0^+(1^{++})$ and that their quark constituents are mainly of the type $n\bar{n}$, where $n = \{u, d\}$. In a previous study of the production rate [2] for the $S = 1$ mesons—which included $^3S_1$, $^3P_0$ and $^3P_2$—an intriguing pattern has been found; it appears that the mesons of the type $^3P_1$, assuming that *both* $f_1(1285)$ and $f_1(1420)$ belong to the category, follow the same pattern. Finally, we conclude that the mesons $\eta(1295)$, $\eta(1440)$ and $h_1(1380)$ are less likely to be produced in the inclusive Z decays compared to $f_1(1285)$ and $f_1(1420)$.

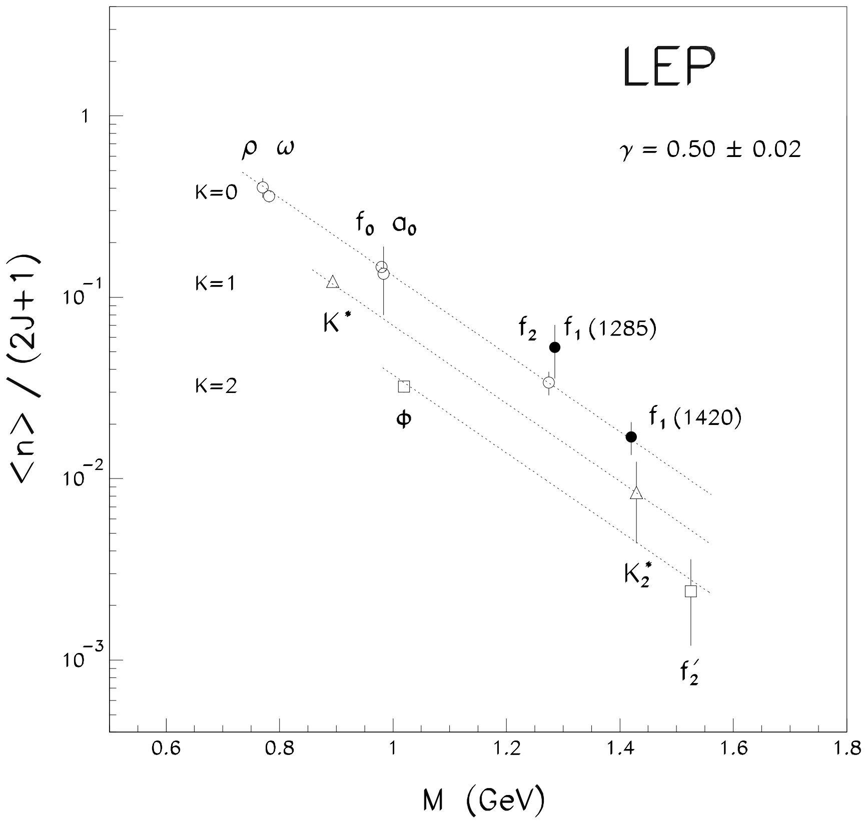

Figure 4: Total production rate per spin state and isospin for scalar, vector and tensor mesons as a function of the mass (open symbols). The two solid circles correspond to the $f_1(1285)$ and the $f_1(1420)$.

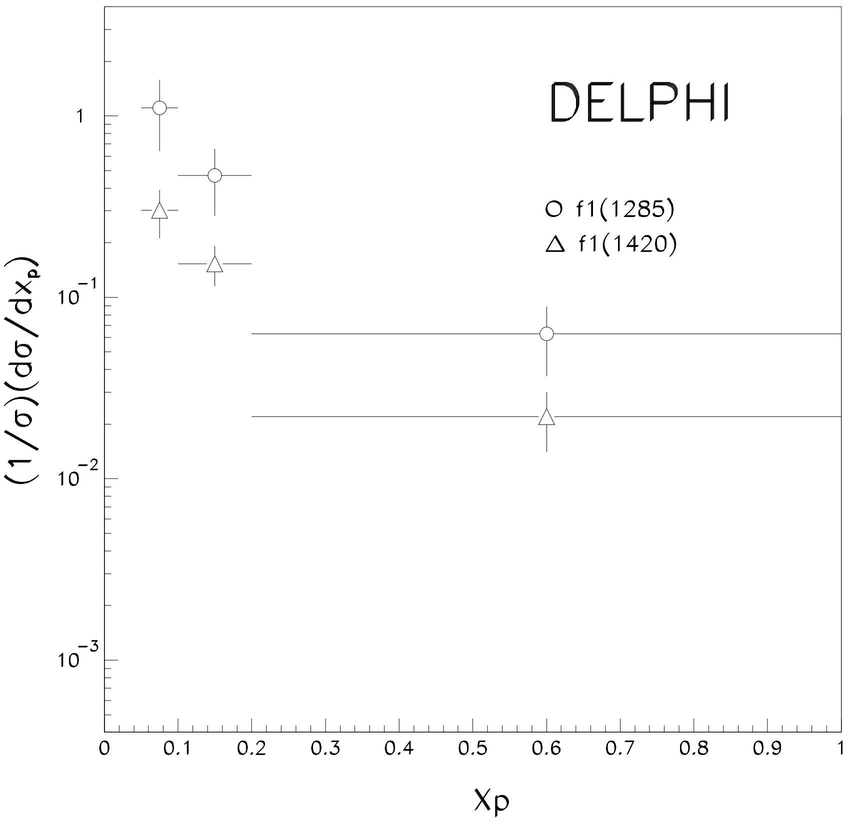

Figure 5: $f_1(1285)$ and $f_1(1420)$ measured differential cross sections. The errors shown are the quadratic sum of statistical and systematic contributions

Acknowledgements

S.-U. Chung is grateful for the warm hospitality extended to him by the CERN staff during his sabbatical year in the EP Division.

References

[1] P. Abreu *et al.*, DELPHI Collab., Phys. Lett. **B449** (1999) 364.
[2] V. Uvarov, Phys.Lett. B511 (2001) 136.
[3] Review of Particle Physics, Eur. Phys. J. C**15**, (2000) 1.
[4] P. Aarnio *et al.*, DELPHI Collab., Nucl. Inst. Meth. **A303** (1991) 233.
[5] P. Abreu *et al.*, DELPHI Collab., Nucl. Inst. Meth. **A378** (1996) 57.
[6] T. Sjöstrand, Comput. Phys. Comm. **82** (1994) 74.
[7] P. Abreu *et al.*, DELPHI Collab., Z.Phys. C 73 (1996) 11.
[8] P.Aarnio *et al.*, DELPHI Collab., Nucl. Instr. Meth. A 378 (1996) 57.
[9] P. Abreu *et al.*, DELPHI Collab., Z.Phys. C 65 (1995) 587.
[10] See, for example, S. U. Chung, 'Spin Formalisms,' CERN preprint 71-8 (1971).
[11] S. U. Chung *et al.*, Phys. Rev. **D60** (1999) 092001.